

# DEVELOPMENT OF PROTOTYPE SOUND DIRECTION CONTROL SYSTEM USING A TWO-DIMENSIONAL LOUDSPEAKER ARRAY

Yasuharu Hashimoto, Masahiko Mikawa, and Kazuyo Tanaka

Graduate School of Library, Information and Media Studies, University of Tsukuba

1-2 Kasuga, Tsukuba-shi, 305-8550, Japan

email: {hashi, mikawa, ktanaka}@slis.tsukuba.ac.jp

## ABSTRACT

*This paper proposes an improved method for a sound direction control system based on the boundary surface control principle. In our previous work, numerical simulations showed that a loudspeaker array with a square-matrix configuration and an elliptical configuration of the suppression control points achieved better characteristics than did a conventional straight-line loudspeaker array. Based on this, we try to construct a real prototype, where a crucial problem is that the elliptical configuration of control sensors is impractical for packaging. Therefore, we develop a method to form a practical control sensor arrangement that has a function equivalent to the elliptical boundary of the control points. The feasibility of the method is first confirmed by numerical simulation and then characteristics of the prototype are examined in a real acoustic environment.*

## 1. INTRODUCTION

One of the goals of computer control of the sound propagation direction is to realize a function that provides quality sound to only a specified "listeners' area" while preventing sound propagation to the "outside zone." There are two techniques for achieving this function, and both employ a loudspeaker array. One method is based on the delay-and-sum algorithm [1], and the other is based on the boundary surface control (BSC) principle [2,3,4]. Both methods use control sound sources constructed from loudspeaker arrays and control sensors composed of one reproduction control point and multiple suppression control points. By using the BSC, we showed in our previous work that employing a loudspeaker array with a square-matrix configuration and an elliptical configuration of the suppression control points achieved better characteristics than did conventional loudspeaker array types [5,9]. In this paper, we construct a prototype of a loudspeaker array system that works in a real acoustic environment.

A crucial problem for constructing a prototype is the arrangement of microphones that function as the suppression control points, because an elliptical configuration is impractical for flexible control of the sensor points. Therefore, we develop a method that can form a reasonable sensor configuration equivalent to the elliptical configuration of the suppression control points.

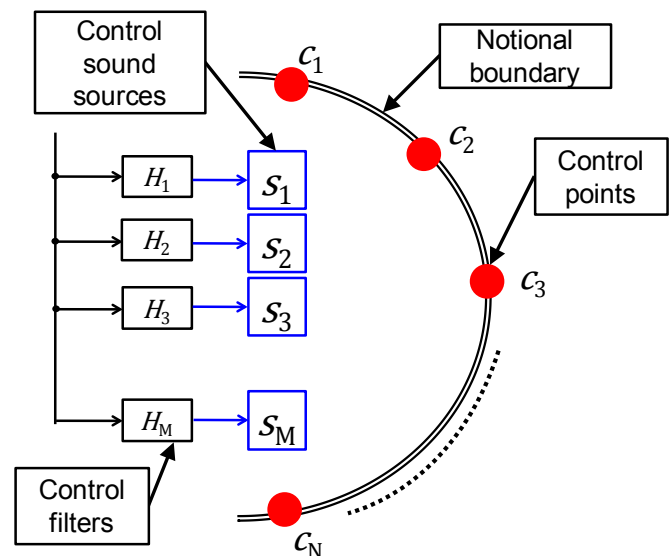


**Fig. 1 Example of the conventional sound field control system based on the BSC : control sound sources (□), suppression control points (●).**

In the following section, we first briefly describe the conventional BSC-based method and then describe the theoretical aspects of the proposed method that can form the equivalent configuration. In Section 3, the design and specification of the prototype system are described. In Section 4, the feasibility of the method is verified by performing numerical simulations for several experimental conditions. Section 5 describes the test results of the prototype system. The conclusion is given in the last section.

## 2. METHOD

### 2.1 BSC-Based Method

According to the BSC principle, the sound field characteristics in a certain area are determined by controlling the values of the acoustic pressure and the particle velocity on the surface boundary enclosing that area. The sound field control system using this principle utilizes the following: sound propagation direction control, active noise control, sound field reproduction, and wave field synthesis.

Figure 1 illustrates an example of the conventional sound field control system based on the BSC. In this example,

a target sound field in the area inside the boundary is controlled by sound control sources. The boundary is a notional boundary that consists of a certain number of control points, as indicated in the figure. The sound pressures on the control points are controlled by the control filters that control the outputs from the loudspeaker array.

The system consists of control sound sources,  $s_m (m = 1, 2, \dots, M)$ , and control points,  $c_n (n = 1, 2, \dots, N)$ . We denote the transfer function from the sound source  $s_m$  to the control point  $c_n$  by  $G_{mn}(\omega)$ , that is

$$\mathbf{G}(\omega) = \begin{bmatrix} G_{11}(\omega) & \cdots & G_{M1}(\omega) \\ \vdots & \ddots & \vdots \\ G_{1N}(\omega) & \cdots & G_{MN}(\omega) \end{bmatrix} \quad (2-1)$$

and the transfer function of the sound control filters by

$$\mathbf{H}(\omega) = [H_1(\omega) \ H_2(\omega) \ \dots \ H_M(\omega)]^T \quad (2-2)$$

When the characteristics of the control points are denoted by

$$\mathbf{A}(\omega) = [A_1(\omega) \ A_2(\omega) \ \dots \ A_N(\omega)]^T \quad (2-3)$$

the following relation holds

$$\mathbf{A}(\omega) = \mathbf{G}(\omega)\mathbf{H}(\omega) \quad (2-4)$$

Here,  $\mathbf{A}(\omega)$  is a given characteristic for the control points from the input.

Then, from Eq. (2-4),  $\mathbf{H}(\omega)$  is obtained

$$\mathbf{H}(\omega) = \mathbf{G}^+(\omega)\mathbf{A}(\omega) \quad (2-5)$$

where + indicates the Moore-Penrose inverse.

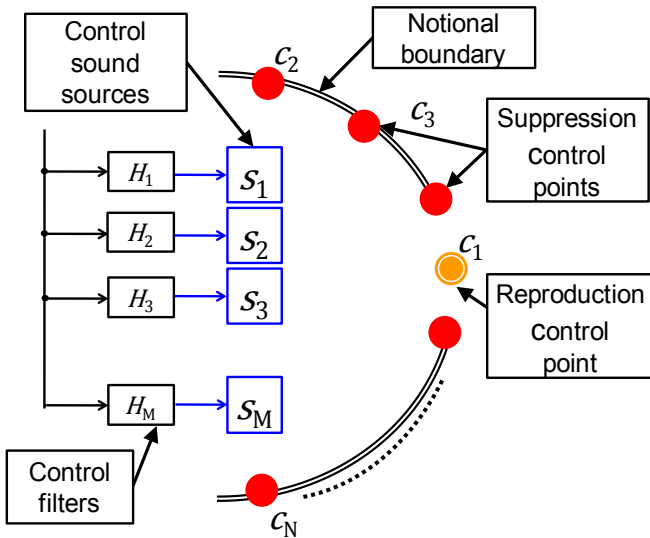


Fig. 2 Sound propagation direction control system applied to the sound field control system: control sound sources (□), reproduction control point (⊙), and suppression control points (●).

The Coefficients of the finite impulse response(FIR) filters for the control filters are derived by taking the inverse Fourier transform of  $\mathbf{H}(\omega)$ .

Figure 2 illustrates the sound propagation direction control system applied to the sound field control system. The system is composed of two types of control points: a reproduction control point that ensures the sound reproduction characteristics, and the suppression control points, located on the notional boundary, that suppress the sound pressure. At the reproduction control point, the element is equal to the system input, and at the suppression control points, the sound pressure should be zero. Therefore,

$$\mathbf{A}(\omega) = [1 \ 0 \ \dots \ 0]^T \quad (2-6)$$

where the first element has the characteristic of the reproduction control point.

## 2.2 Arrangements of the Elliptical Control Points

As described in [5], when employing a circular arrangement as the suppression control boundary, the sound energy is reflected at the boundary and the reflected energy flows to the opposite side of the circle. Thus, the sound energy diffuses in random directions and it is difficult to form a sharp main lobe. To overcome this problem, we introduced an elliptical suppression control boundary, as shown in Fig. 3, where the center of the loudspeaker array is located at one focal point of the ellipse and another focal point is located at the reproduction control point. In this configuration, the sound energy reflected at the boundary accumulates at another focal point. We also verified by numerical simulations that the elliptical boundary for the suppression control points suppresses the side lobes of the directivity.

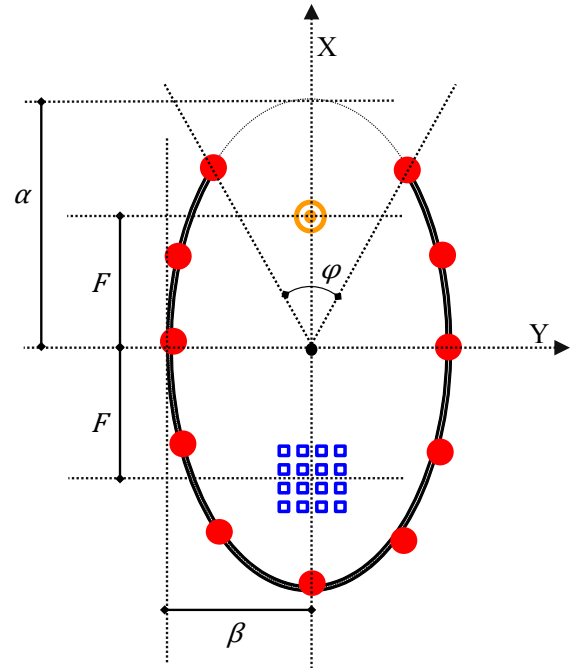
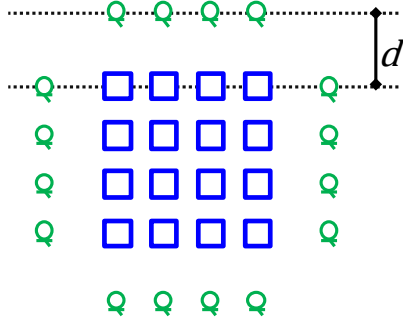


Fig. 3 Arrangement of the elliptical control points: control sound sources (□), reproduction control point (⊙), suppression control points (●), and aperture angle  $\phi$ .



**Fig. 4 Practical arrangement of the microphones: control sound sources (  $\square$  ), and microphones (  $\circ$  ).**

### 2.3 Method of Forming the Equivalent Control Points

For sound field control based on the BSC, the values of the transfer function from the sound sources to the control points  $\mathbf{G}(\omega)$  must be determined. That is, the impulse response must be measured at the microphones on the control points to obtain  $\mathbf{G}(\omega)$ . However, it is not practical to locate microphones at the control points on the elliptical boundary, for the following reasons:

- 1) the elliptical boundary has a curved shape, and
- 2) the arrangement is different in individual directivities.

Therefore, we propose a method for forming a practical microphone arrangement that has a function equivalent to the elliptical boundary of the control points.

Figure 4 shows one of the practical arrangements of microphones, where the microphones are arranged on a line symmetrically with each directivity. We denote the transfer function from the sound source  $s_m$  to the control point  $v_l$  ( $l = 1, 2, \dots, L$ ) by  $K_{ml}(\omega)$ , that is

$$\mathbf{K}(\omega) = \begin{bmatrix} K_{11}(\omega) & \cdots & K_{M1}(\omega) \\ \vdots & \ddots & \vdots \\ K_{1L}(\omega) & \cdots & K_{ML}(\omega) \end{bmatrix} \quad (2-7)$$

where  $\mathbf{K}(\omega)$  is obtained by measurement. Here, we satisfy the characteristic of each microphone  $v_l$ . All elements are assumed to be in the free sound field. The transfer function from the sound source  $s_m$  to the control point  $c_n$ , denoted by  $\hat{G}_{mn}(\omega)$  is given by

$$\hat{G}_{mn}(\omega) = \frac{1}{4\pi r_{mn}} e^{-j\omega \frac{r_{mn}}{c}} \quad (2-8)$$

where  $c$  is the sound velocity and  $r_{mn}$  is the distance between the sound source  $s_m$  and the control point  $c_n$ . Then, the estimates of the control filter  $\hat{\mathbf{H}}(\omega)$  are calculated by  $\mathbf{A}(\omega)$  in Eq.(2-6) and the transfer function  $\hat{\mathbf{G}}(\omega)$  in the free sound field. Similarly, the free-field-assumed transfer function  $\hat{\mathbf{K}}(\omega)$  from the sound source  $s_m$  to microphone  $v_l$  is given. At the same time, by using the estimated control filter  $\hat{\mathbf{H}}(\omega)$ , the transfer function  $\mathbf{F}(\omega)$  from the input to the microphones  $v_l$  is given by

$$\mathbf{F}(\omega) = \hat{\mathbf{K}}(\omega) \hat{\mathbf{H}}(\omega) \quad (2-9)$$

Here, by using the configuration of the elliptical control points in the free sound field,  $\mathbf{F}(\omega)$  has the characteristics of microphone  $v_l$  that satisfy the sound propagation direction control. From  $\mathbf{F}(\omega)$  and  $\mathbf{K}(\omega)$ , which can be measured, control filter  $\mathbf{H}(\omega)$  is given by

$$\mathbf{H}(\omega) = \mathbf{K}^+(\omega) \mathbf{F}(\omega) \quad (2-10)$$

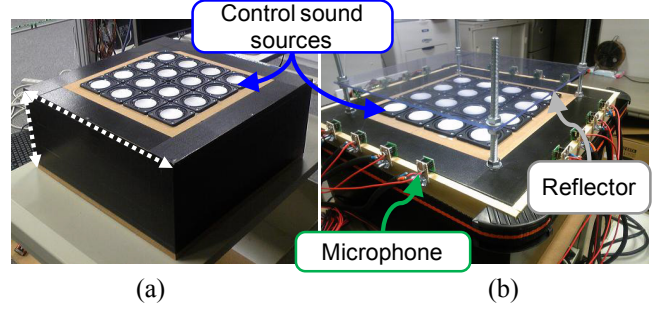


**Fig. 5 Prototypes of the loudspeaker array: (a) Simple, (b) Equipped with a reflector and microphones**

## 3. PROTOTYPING OF THE LOUDSPEAKER ARRAY

### 3.1 The System Design

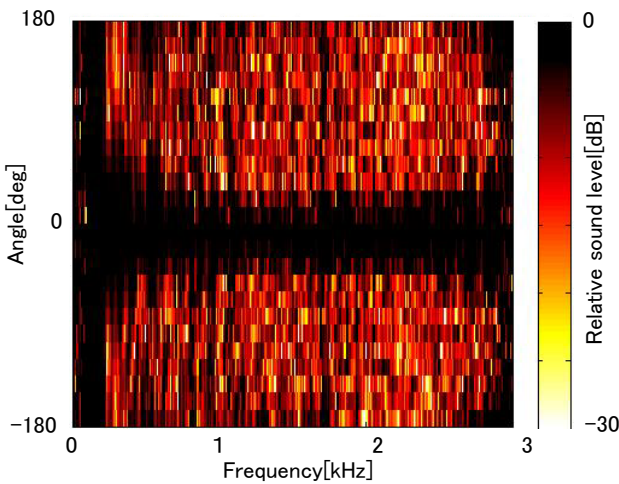
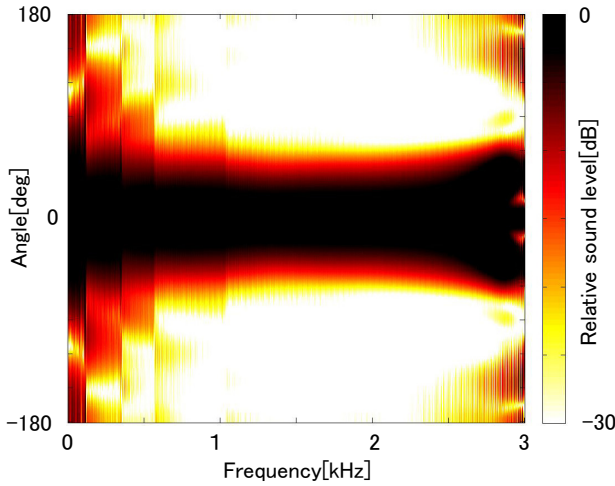
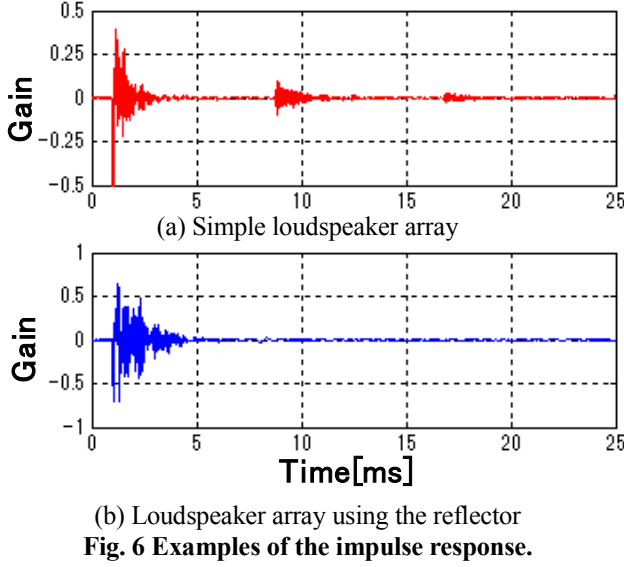
Figure 5(a) illustrates the prototype of the loudspeaker array. The configuration of the loudspeaker is a square-matrix array. As confirmed in the previous paper, this configuration enables high directivity for a small number of loudspeakers and it is simple and easy to locate on a real plane. The array consists of 16 ( $4 \times 4$ ) loudspeakers, each of which is separated by an interval of 60 mm.

### 3.2 Measurement of the Impulse Response and the Improvement by the Reflector

For the prototypes shown in Figs. 5(a) and (b), the impulse responses at the microphones from individual sound sources were measured. The arrangement of the microphones is shown in Fig. 4 and the distance between each microphone and the outside line of the sound sources was 10 cm.

Figure 6(a) shows an example of the impulse response of the simple prototype. Two peak waveforms appear in addition to the initial response. The second peak is delayed for approximately 8.3 ms after the first peak, and this time delay corresponds to approximately 2.8 m. Because the distance between the unit and the ceiling in the experimental environment was approximately 1.4 m, this peak is considered to be a reflection wave from the ceiling. The reflection from the ceiling was changed by the ceiling material and the distance, and so the reflection caused performance degradation of the directivity.

To avoid this degradation, we installed a reflector to prevent the reflection from the ceiling, as shown in Fig. 5(b). Figure 6(b) shows an example of the impulse response obtained by the prototype with the reflector. In this case, no reflected wave is observed. The gain of the initial response is approximately two times the gain in Fig. 6(a). Thus, the reflector also increased the output in the two-dimensional plane.



## 4. NUMERICAL SIMULATION

The validity of the proposed method for forming the equivalent control points was examined in a free sound field by numerical simulation.

### 4.1 Experimental Conditions

In this case, the measured  $K(\omega)$  value is assumed to be equal to  $\hat{K}(\omega)$  the calculated value from Eq. (2-8). The configuration of the control sound sources and the microphones are the same as those used in the measurement of the impulse response described in Section 3. The angle of 0 degrees indicates the direction of the x-axis in Fig. 3. The direction of the main lobe is specified as 0 degrees in the experiments. Following the arrangement shown in Fig. 3, 511 notional suppression control points are located on the elliptical boundary, where  $F = 0.5$  m,  $a = 1.0$  m,  $b = 1.3$  m,  $\phi = 180$  degrees. The control filters are constructed by 512-tap FIR filters. The sampling frequency is 6 kHz.

### 4.2 Results

Figure 7 shows the acoustic pressure distributions of the proposed method as obtained by the numerical simulation. This result and that obtained from the system which has no microphones are in good agreement. Thus, it was confirmed that the control points by Eq. (2-9) are equivalent to those by Eq. (2-10). Moreover, only the main lobe direction has high sound pressure; this result indicates the effectiveness of the directional control method using the elliptical control points.

## 5. EXPERIMENTS IN A REAL ENVIRONMENT

### 5.1 Experimental Conditions

The configurations of the loudspeakers and the microphones are essentially the same as those used in the numerical simulation described in Section 4. The impulse responses are measured by using the time stretched pulse (TSP). The measurement points are located on the circumference of a 50 cm radius circle at intervals of 15 degrees. We evaluated the following three conditions.

- 1) Comparison of the measured and the predicted values:  
The case of using the control filter  $H(\omega)$  and another case of using the predictive control filter  $\hat{H}(\omega)$  calculated from the transfer function in the free sound field are compared.
- 2) Directivity performance evaluation within the range of symmetry:  
The results of each main lobe direction (0, 15, 30, 45 degrees) are compared.
- 3) Evaluation of the symmetry of the square-matrix array:  
The results of main lobe direction (0, 90, 180, -90 degrees) are compared.

### 5.2 Results

Figure 8 shows the acoustic pressure distributions measured in the real environment based on the proposed method. These results show good agreement with the result of the numerical simulation shown in Fig. 7, although the depressions somewhat decreased.

Figure 9 shows the comparative results of the measured and the predicted values. The difference of the suppressive effect between the measured and predicted values is ap-



proximately 4 dB; this result indicates the validity of using the measured value. Figure 10 shows the results of the directivity performance within the range of symmetry. Each direction of the main lobe has a maximum sound pressure in each target direction. These results indicate that the desired direction pattern can be obtained.

Figure 11 shows the results of evaluating the symmetry of the square-matrix array. Each direction of the main lobe in the 90 degree interval has similar directivity. From the above three evaluations, shown in Figs. 9, 10 and 11, it is confirmed that the directivity can be formed in at least 15 deg intervals. However, the performance for the multiple bands is degraded, as shown in Fig. 8.

## 6. CONCLUSION

We constructed a prototype of a square-matrix loudspeaker array system for sound directivity control. Our system employed elliptical control points based on the BSC principle. To construct the system in real space, we proposed a method to form a practical microphone arrangement equivalent to the arrangement of the elliptical control points. The performance of the proposed method was confirmed by experiments in a real environment and showed that the directivity can be formed in various directions by the proposed system.

## ACKNOWLEDGEMENT

This research is supported in part by a Grand-in-Aid for Scientific Research, Project No.22500145, from the Japan Society for the Promotion of Science.

## REFERENCES

- [1] P.A. Nelson, "Active control of acoustic fields and the reproduction of sound," J. Sound and Vibration, 177, pp.447-477, 1994.
- [2] N. Epain, E. Friot, "Active control of sound inside a sphere via control of the acoustic pressure at the boundary surface," J. Sound and Vibration, 299, pp.287-604, 2007.
- [3] S. Ise, "The Boundary Surface Control Principle and Its Applications," IEICE Trans. on Fundamentals of Electronics, Communications and Computer Sciences, E88-A(7), pp.1656-1664, 2005.
- [4] S. Enomoto, S. Ise, "A proposal of the directional speaker system based on the boundary surface control principle," Electronics and Communication in Japan (part III: Fundamental Electronics Science), Wiley Periodicals, Vol. 88, Issue 2, pp. 1-9, 2005.
- [5] Y. Hashimoto, M. Mikawa, K. Tanaka, "A Flexible Method for Sound Propagation Direction Control Based on the Boundary Surface Control Principle," Proc. of Inter-noise 2008, Paper No. 0239 (8 Pages), 2008.
- [6] S. Spors and R. Rabenstein, "Spatial aliasing artifacts produced by linear and circular loudspeaker arrays used for wave field synthesis," in 120th Convention of the AES, Paris, France, May 20-23 2006.
- [7] E. Mabande, W. Kellermann "Towards Superdirective Beamforming with Loudspeaker Arrays," Conf. Rec. International Congress on Acoustics, Madrid, Spain, Sep. 2007

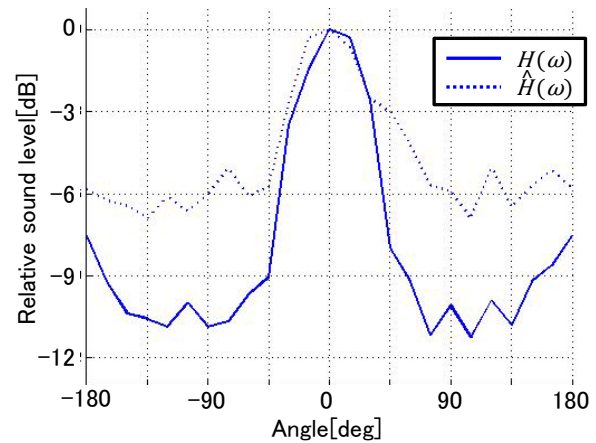


Fig. 9 Directivity characteristics estimated for 0-degree main lobe direction.

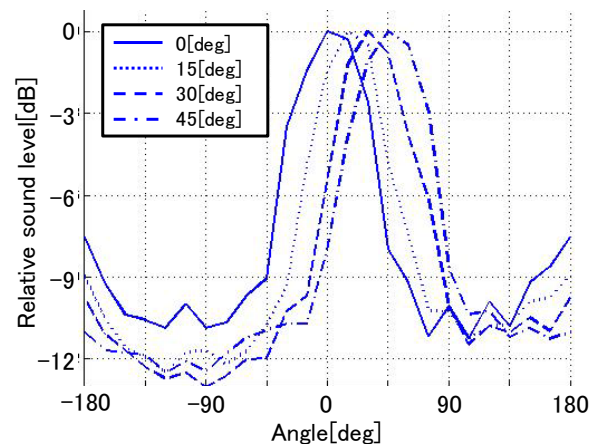


Fig. 10 Directivity characteristics estimated for each main lobe direction (0, 15, 30, 45 degrees).

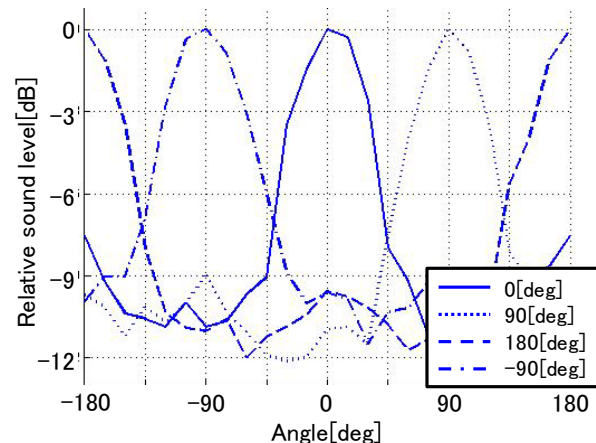


Fig. 11 Directivity characteristics estimated for each main lobe direction (0, 90, 180, -90 degrees).

- [8] T. Nakashima, S. Kim, K. Imoto, S. Ise, "Effect of active noise reflection unit (ANRU) on noise reduction," (in Japanese) J. Acoust. Soc. Japan, Vol. 65, No. 9, pp. 461-468, 2009.

- [9] Y. Hashimoto, M. Mikawa, K. Tanaka, "Sound propagation direction control using three configurations of two dimensional loudspeaker array," Proc. of EUSIPCO2010, pp.1958-1962, August 2010.